ORIENTAL JOURNAL OF CHEMISTRY
An International Open Access, Peer Reviewed Research Journal
www.orientjchem.org
Est. 1984

ISSN: 0970-020 X
CODEN: OJCHEG
2023, Vol. 39, No.(5):
Pg. 1255-1263

Photocatalytic Degradation of Azo Dyes by Zinc Oxide Nanoparticles Fabricated using Aqueous Flower Extract of *Cassia alata*

S. KARTHIKA[1], N.MANI[1], K. ANNAIDASAN[2], LATHA MAHESWARI[1], and N. KAVIKALA[1]

[1]Department of Chemistry, A.V.V.M Sri Pushpam College (Affiliated to Bharathidasan University), Poondi, Thanjavur (Dt), Tamil Nadu, India.
[2]Department of Geography, Central University of Tamilnadu, Thiruvarur, India.
*Corresponding author E-mail: karchemistry28@gmail.com

http://dx.doi.org/10.13005/ojc/390519

(Received: August 01, 2023; Accepted: October 02, 2023)

ABSTRACT

The Industrial Revolution can lead the economic development across the globe, and it also causes severe environmental and water. Among the various types of pollutants, industrial dyes pose a serious threat to public health. Hence, remediation of these toxic dyes from water sources has become highly essential in terms of public health. The present study focused on the use of nanoparticles synthesized using plant sources for the remediation of azo dyes such as Methyl orange (MO) Congo red (CR), Malachite Green (MG), Eriochrome Black T (EBT) under direct solar radiation. The fabrication of Zinc oxide nanoparticles (ZnO-NPs) was mediated by aqueous flower extract of Cassia alata. The synthesized nanoparticles exhibited a surface plasmon resonance (SPR) vibration at wavelength 372 nm. The FTIR analysis revealed aromatic amines and alcohols coating the surface of ZnO-NPs. The XRD analysis showed that the synthesized nanoparticles are highly crystalline and possess hexagonal wurtzite structures. The particle size measured with maximum diffraction peak using Scherrer's equation was 9.93 nm. The SEM images showed spherical morphology. The particle size determined with Dynamic Light Scattering (DLS) was 78.18 nm and the zeta potential analysis showed that the ZnO-NPs was -14.6 mV, indicating good dispersion and stability. The C.alata mediated ZnO-NPs exhibited excellent Photocatalytic degradation of azo dyes. Degradation efficiency of Methyl orange, Malachite green and Eriochrome black T are 76.65%, 65.07%, 60% respectively at 150 minute. But Congo red is 72.76% at 120 min, because the Congo red was completely degraded at 120 minute. The study shows that green mediated ZnO-NPs could be effectively used as an eco-friendly alternative for the remediation of chemical pollutants from water.

Keywords: *Cassia alata*, Zinc oxide nanoparticles, Methyl orange, Congo red, Malachite Green, Eriochrome Black T, Photocatalytic degradation.

INTRODUCTION

Water is an inevitable resource for the sustenance of all life forms on Earth. The swift industrial growth in developing countries emanates fromwater pollution due to organic and inorganic

pollutants. Dyes are one such organic compound that churns out colour due to its ability to absorb light when dissolved in water. They are enduring organic pollutants released from the textile, paper, pharmaceutical, tannery and dyeing industries. The textile industries extensively utilizes azo dyes which are categorized by the presence of functional group –N=N attached to aromatic moieties. The Azo dyes are synthetic colourants and approximately 20 to 25% of the dyes vanish during dyeing processes and settle in the environment when discharged without proper treatments. These dyes, when discharged into water bodies, even at very low concentrations, are persistent and recalcitrant. The complex structure and their stability make them non-biodegradable[1,2]. Further, they are also mutagenic and carcinogenic. Hence, the removal of these organic dyes from water sources is highly important[3]. A number of physical and chemical methods are conventionally employed for the degradation of dyes. The physical processes end up in transferring the pollutants from one medium to another resulting in secondary pollutants. The chemical methods for the degradation of organic pollutants produce enormous amounts of sludge and are also expensive. The biological treatments of dye substances are ineffective because of their resistance to aerobic decolourization and anaerobic treatment of azo dyes results in the generation of aromatic amines that are carcinogenic[4,5]. Hence, the search for an environmentally friendly and non-toxic alternative is essential.

The current research developments focus on the photocatalytic degradation of organic dyes utilizing semiconductor nanoparticles. In this study, the green chemistry approach for the synthesis of nanoparticles has been adopted. The n-type semiconductor, Zinc oxide nanoparticles (ZnO-NPs) was synthesized using aqueous flower extract of Cassia alata. This green mediated ZnO-NPs was employed for the degradation of azo dyes due to its high photo sensitivity, non-toxic nature, cost effectiveness in fabrication, wide band gap, high photocatalytic and quantum efficiency[6,7]. Further, they can be easily scaled up for large scale production. In the present study, Methyl Orange, Congo Red, Malachite Green and Eriochrome Black T are used as model dye. Methyl orange is used as an indicator in titrations due to its ability to produce variations in colour at different pH8. It is used as colouring agents in food, pharmaceuticals, leather and textile industries. Congo red is an anionic diazo dye that produces carcinogens such as benzidine[9]. This dye is commonly employed in the silk manufacturing industries. Malachite green is a synthetic triphenyl methane dye and has applications in textile, fisheries and dyeing industries[10,11]. Eriochrome Black T is an anionic dye used in the determination of water hardness. It is used in the paper, pharmaceutical, textile industries and also in research laboratories[12]. These organic dyes are carcinogenic, mutagenic and are not easily degradable[13,14]. Further, they are persistent and highly resistant to biological degradation due to the presence of aromatic and sulphonate groups[15,16].

C. alata (Fabaceae) is a medicinal plant used in traditional medicine in India and South East Asia[17]. The plant is rich in phytochemicals such as flavonoids, alkaloids, tannins, triterpenoids, anthroquinones and sterols[18,19]. The presence of biomolecules such as proteins and carbohydrate (reducing sugars) together with secondary metabolites play an effective role of stabilizer in the fabrication of ZnO-NPs[20,21]. Thus, the objective of the present study is to synthesis ZnO-NPs using aqueous flower extract of *C. alata* for the photocatalytic degradation of azo dyes.

MATERIALS AND METHODS

Materials

Bright yellow coloured *C.alata* flowers were collected from Thanjavur, Tamilnadu, India. They were taxonomically identified atthe department of botany, St. Joseph's College, Tiruchirappalli, Tamilnadu, India.The chemicals used in this study are analytical grade chemicals procured from Sigma- Aldrich Pvt. Ltd.

Synthesis of ZnO-NPs

The shade dried flower powder of *C.alata* (5 g) was dissolved in 100 mL of double distilled water to prepare a 5% aqueous flower extract by boiling for 10 min at 70°C. 10 mL of this aqueous flower extract was filtered using Whatmann filter paper no.1 and added to 50 mL of zinc nitrate solution (0.1M). The flower extract and metal precursor solution was boiled for 2 h at 75°C. After boiling, the supernatant was discarded and the pale white precipitate formed by centrifuges to 1000 rpm for 10 min with the addition of distilled water. The

pellets were collected, dried in an oven for 12 h and calcinated at 350°C for 2 hours[22].

Characterization of ZnO-NPs

The surface plasmon resonance (SPR) of ZnO-NPs was monitored using UV-Visible spectroscopy at wavelength between 200 and 800 nm. The FTIR absorption spectrum of ZnO-NPs was recorded between 400 and 4000 cm^{-1} in diffuse reflectant mode to identify the functional groups present on the surface of synthesized nanoparticles. The crystallinity and particle size of the nanoparticles were determined using X-ray diffraction spectroscopy. Debye-Scherrer's equation ($L=0.9\lambda/\beta\cos\theta$) was used for calculating the particle size. The morphology and elemental composition of the nanoparticles were determined using SEM and EDAX analysis. The particle size and surface charge of ZnO-NPs was determined with DLS and zeta potential analysis.

Photocatalytic activity of ZnO-NPs

Methyl orange, congo red, malachite green, and Eriochrome Black T dyes were used as a model system for studying the photocatalytic activity of the ZnO-NPs in the presence of direct sunlight. 1000 ml of distilled water was combined with 15 mL of dye. 0.1 g/L of plant extract-mediated nanoparticles received 100 mL of dye (ZnO-NPs). A control was maintained without the addition of nanoparticles. Before exposing the combination to direct sunlight irradiation, the mixture was magnetically agitated for 30 min in a dark environment. 2 mL of the solution was centrifuges at 10,000 rpm for 10 min at predetermined intervals (every 30 min) to get a clear supernatant, and the optical density was assessed using a UV-visible spectrophotometer in the wavelength range of 300 to 800 nm[23,24]. The λ_{max} of dye was detected at 460 nm (Methyl orange), 480 nm (Congo red), 618 nm (Malachite green), and 530 nm (Eriochrome Black T). By measuring the absorbance of dye, the concentration of dye following photocatalyticdegradation was assessed using the following equation[25,26].

$$\text{Dye degradation (\%)} = \frac{\text{Ao} - \text{At}}{\text{Ao}} * 100$$

RESULT AND DISCUSSION

The development of industrialization at a rapid phase has led to enormous amounts of pollutants and, in turn to environmental toxicity. The discharge of synthetic dyes from various industries into drinking and fresh water sources causes water toxicity[27,28]. The exorbitant use of coloured substances, particularly in the textile sector, has led to serious ecological problems[29]. Among the different classes of coloured substances used in industries, azo dyes are the most important dye that is being utilized above 80% in comparison to other classes of dyes[30]. Metal oxide nanoparticles act as catalysts in the degradation of dyes. ZnO nanoparticles are metal oxide nanoparticles that have a band gap of 3.3 eV and excitation binding energy of 60 meV[31,32]. The photocatalytic activity of ZnO-NPs is due to their large surface area to volume ratio[33,34].

10 mL of 5% aqueous flower extract of *C. alata* was mixed with 50 mL of 0.1 N zinc nitrate solution and heated to 75°C for 2 hours. The light brown colour of the solution turned into a pale white colour, indicating the formation of ZnO nanoparticles. A small fraction of the dried and calcinated powder of *C. alata* mediated ZnO-NPs was examined using UV-spectroscopyat a wavelength ranging between 200 to 800 nm exhibited a surface plasmon resonance peak at a wavelength measuring 372 nm Fig.1. *Kalopanax septemlobus* mediated ZnO-NPs exhibited a surface plasmon resonance at wavelength 372 nm[35,36] was in agreement with the present study. The ZnO-NPs prepared using Eucalyptus globulus leaf extract exhibited an absorption peak at 375 nm, indicating the characteristics SPR of ZnO-NPs[37]. The formation of a sharp peak confirms the presence of mono-dispersed ZnO-NPs[38]. The absorption peak obtained with *C. alata* flower extract mediated ZnO-NPs was lower compared to its bulk material, ZnO given as 380 nm[39].

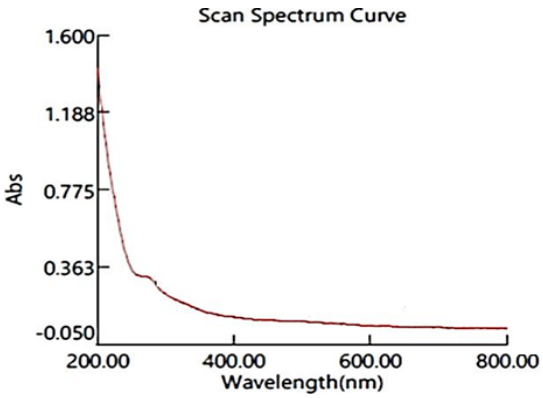

Fig. 1. UV absorption spectrum of C.alata mediated ZnO-NPs

The FTIR spectrum of *C. alata* aqueous flower extract medicated ZnO-NPs Fig. 2 exhibited prominent peaks at the stretching vibrations of the OH group was assigned with the peak at 3417.01 cm^{-1} [40,41]. The peak representing the C-H stretching vibrations due to CH_2 group was shown at 2919.58 cm^{-1} [42]. The presence of C=O group was indicated by the peak at 2850.88 cm^{-1} [43]. The peak at 1605.97 cm^{-1} shows the carboxyl group symmetric stretching vibrations of aminoacids present in the protein molecules[44]. The C=O stretching vibrations of the carboxylic group was represented with the peak at 1518.80 cm^{-1} [45]. The peak at 1410.79 cm^{-1} indicates the C-N stretching present in aminoacids[46]. The C-N stretching of aromatic amines was indicated with the peak at 1252.63 cm^{-1} [47,48]. The synthesis of ZnO-NPs and the zinc oxide bond was shown with peaks at 1193.24 cm^{-1}, 693.15 cm^{-1}, 658.03 cm^{-1}, 643.82 cm^{-1}, 602.00 cm^{-1}, 536.44 cm^{-1} and 470.79 cm^{-1} 49,50. The C-O stretching vibrations and the C=C stretching vibrations of aromatic amines was represented with peak at 1098.64 cm^{-1} and 1036.23 cm^{-1} [51]. The C-H vibration was indicated with the peak at 836.71 cm^{-1} [52]. The presence of aliphatic chloro compounds was shown with the peak at 777.58 cm^{-1} [16,20,48,52]. Thus, from the FTIR spectrum it was identified that functional groups OH, NH, $-CH_2$, C=C, C-O of aromatic amines and alcohols and are involved in the reduction of zinc ions and in the stabilization of ZnO-NPs.

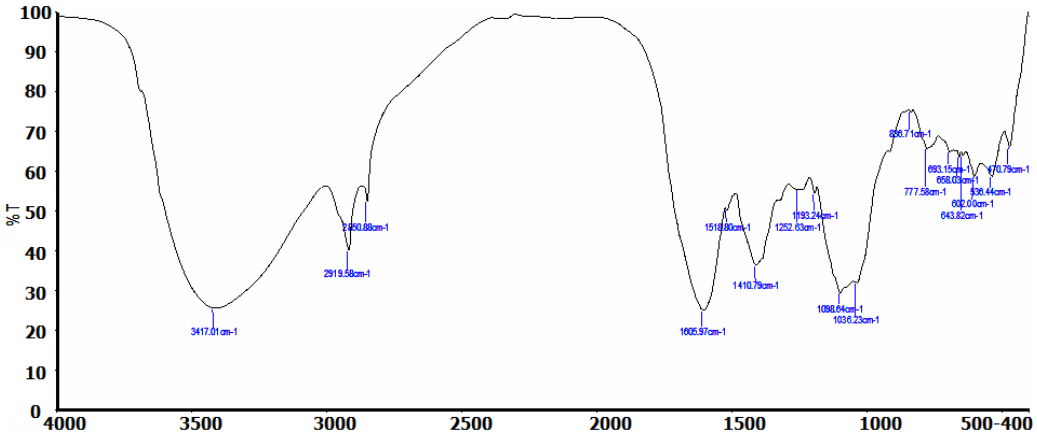

Fig. 2. FTIR spectrum of *C. alata* mediated ZnO-NPs

C. alata aqueous flower extract mediated zinc oxide nanoparticles were subjected to XRD analysis for the confirmation of nano synthesis and to identify the crystallinity and size. The zinc oxide nanoparticles exhibited prominent De Bragg's reflection values of 31.66°, 34.33°, 36.21°, 47.63°, 56.48°, 62.61°, 67.95° and 69.17° when recorded at 2 angles from 10 to 90°. The De Bragg's reflections corresponded to the crystalline plane index (100), (002), (101), (102), (110), (103), (112) and (201) Fig. 3. These planes of indices confirm the synthesis of hexagonal phase (Wurtzite) zinc oxide nanoparticles. The broadening of peaks and noise visualized might be probably due to nanosized particles and biomolecules. The XRD spectrum matched the standard diffracted powder card no. JCPDS No 089-0511. it has reported a XRD peaks for ZnO-NPs synthesized using bark extract of Aglaiaelaeagnoidea that was in agreement with this study. The average size of the nanoparticles calculated with major diffraction peak using Scherrer's equation was 9.93 nm.

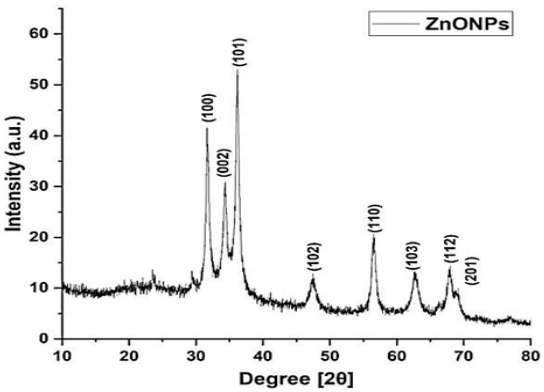

Fig. 3. XRD Diffractogram of *C. alata* mediated ZnO-NPs

The SEM micrograph of the synthesized ZnO-NPs was found to contain hexagonal wurtzite structures with high crystallinity and uniform distribution Fig. 4. The particles were found to

be agglomerated and the EDX pattern revealed the composition of nanoparticles which reported 64.81% of zinc, and 24.12% of oxides Fig. 5. The SEM micrograph shows that the particles were agglomerated, a typical phenomenon observed in green synthesis of nanoparticles. The aggregation of nanoparticles might be attributed to the large surface area to volume and due to the affinity of nanoparticles towards each other[4,6,48,52]. The ecological factors are highly influential for the stability and agglomeration of nanoparticles during their synthetic process and form asymmetric clusters[20,40].

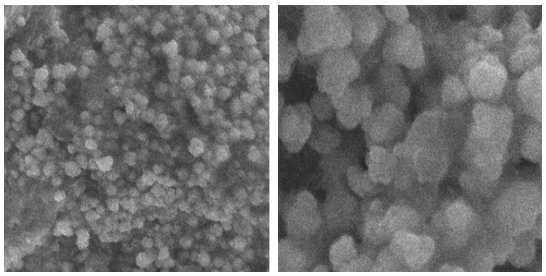

Fig. 4. SEM micrograph of *C. alata* mediated ZnO-NPs

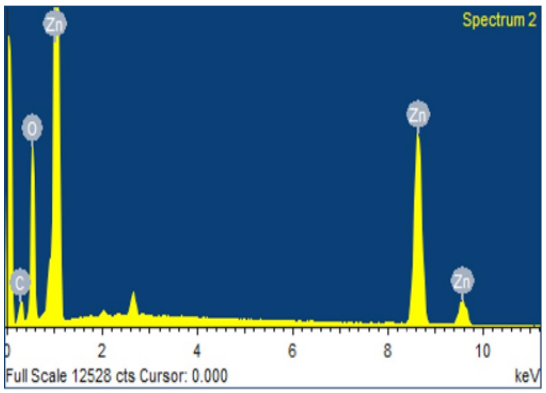

Fig. 5. EDAX spectrum of *C. alata* mediated ZnO-NPs

The determination of particle size using Debye-Scherrer's equation is best suited for semispherical and spherical structures. Hence, to obtain a more precise particle size, Dynamic Light Scattering (DLS) analysis was performed. DLS analysis indicated that the particle size was 78.18 nm Fig. 6. DLS provides a much larger value of particle size due to its hydrodynamic shell, which is dependent on the structure, shape and roughness of the synthesized nanoparticles (Katzel *et al.,* 2008). The surface charge and the stability of ZnO-NPs were evaluated with zeta potential analysis. The surface charge of the nanoparticles was -14.6 mV Fig. 7 as observed with zeta potential analysis.The results indicated that the ZnO-NPs were coated with negatively charged groups, which account for its moderate stability[16,35].

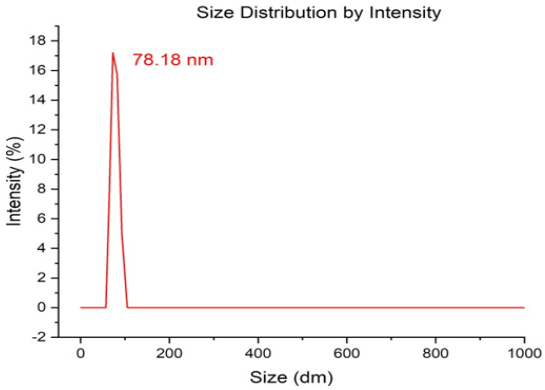

Fig. 6. DLS analysis of *C.alata* mediated ZnO-NPs

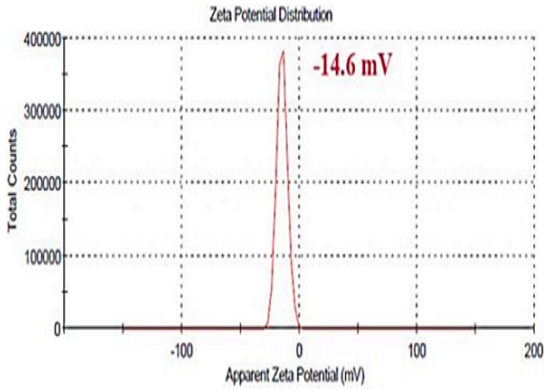

Fig. 7. Zeta potential analysis of *C. alata* mediated ZnO-NPs

C. alata mediated ZnO-NPs exhibited 76.65%, 72.76%, 65.07% and 60% of degradation of methyl orange, congo red, malachite green and Eriochrome Black T dye respectively Fig. 8 and Table 1. The absorption bands with high intensity are found at 460 (M.O), 486 (CR), 618 (MG) and 530 nm (EBT). Among the evaluated dyes, Congo red was degraded to 72.76% within 120 minute. Maximum intensity of absorption peak was observed at 0 min followed by a drastic decrease in intensity of peak after 30 min, which might have resulted in complete saturation of dye molecules within 30 min of exposure and due to affinity of nanoparticles towards dye molecules[20,51]. The Photocatalytic acceleration of MO degradation was 85% in 180 min of exposure to nanoparticles[34,35,41] reported 100% degradation of MO in 240 min by ZnOnanoflowers synthesized using precipitation method. The ZnO-NPs synthesized using aqueous extract of Amomumlongiligulare showed a decrease in the concentration of malachite

green dye with a decrease in its characteristic peak at 619 nm. After 60 min of photocatalytic activity, 38.1% of dye degradation[37] was in agreement with the present study. Similarly, 35 reported 90% of EBT degradation in 5 h by ZnO-NPs, whereasthe present study reported 60% within 150 minute. When the nanoparticles are irradiated by a light source, electrons present on the surface of the nanoparticles get excited from valance band to conduction band utilizing the energy of light source (Photoexcitation). The dissolved oxygen in the reaction mixture utilizes photo excited electrons for the formation of oxygen free radicals. Simultaneously, the photoexcited holes produced in the valence band oxidises the water molecules that have been absorbed and produce OH radicals. Both the superoxide and hydroxyl radicals with high oxidation co-efficient react with dye molecule and degrade it into their by-products[20,34,35].

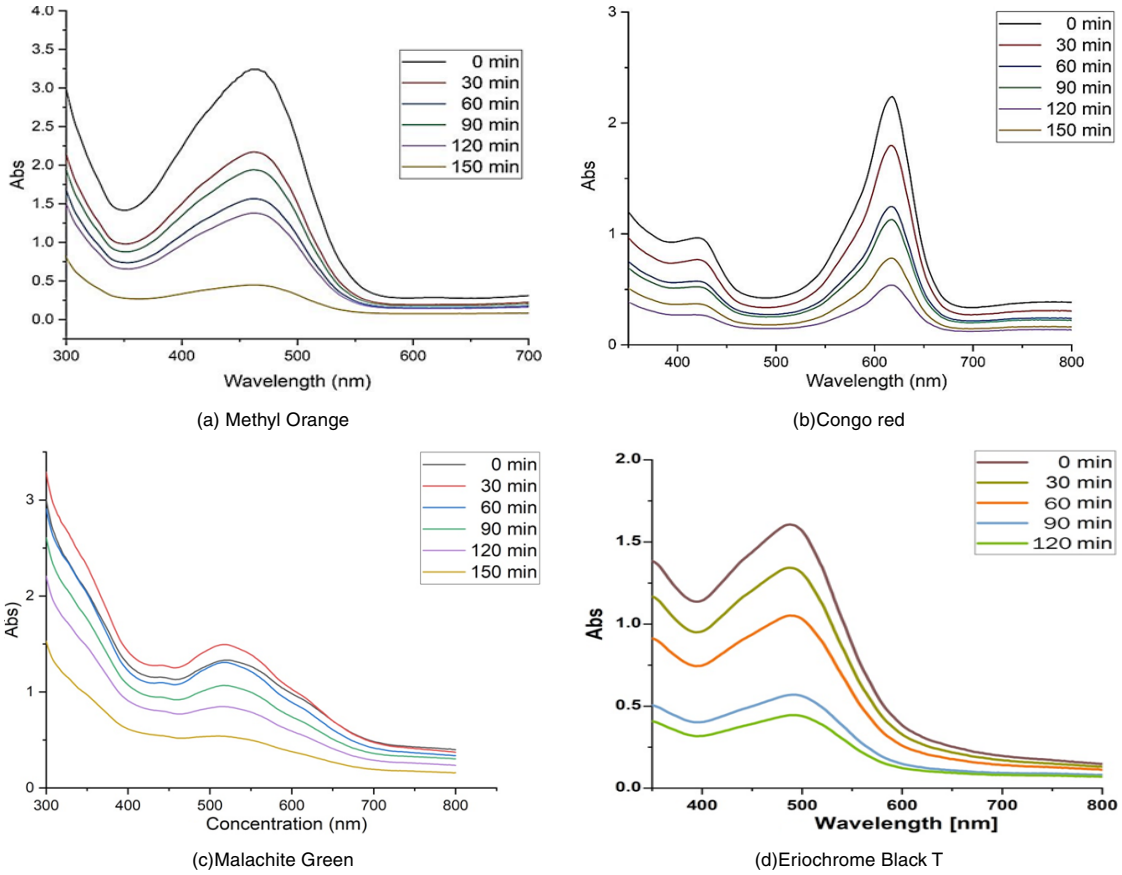

Fig. 8. Photocatalytic degradation of azo dyes by *C.alata* mediated ZnO-NPs

Table 1: Photocatalytic degradation (%) of azo dyes by ZnO-NPs

Sl. No	Dye	Reaction time (Min)	% of Degradation
1	Methyl orange	150	76.65
2	Congo Red	120	72.76
3	Malachite Green	150	65.07
4	Eriochrome Black T	150	60

CONCLUSION

The study witnessed the successful synthesis of ZnO-NPs using aqueous flower extract of *C.alata*. The synthesized nanoparticles possessed hexagonal wurtzite shapes with an average particle size of 78.18 nm as given by DLS measurements. The Green chemistry mediated ZnO-NPs was effective as the fabrication of nanoparticles with a particle size of less than 100 nm was achieved. Due to the non-toxic and biocompatibility nature of ZnO-NPs it could be utilized in a wide range of applications. In the present work, ZnO-NPs exhibited effective Photocatalytic activity as > 60% of degradation of dyes was achieved with the evaluated dyes. ZnO-NPs showed maximum activity against methyl orange and congo red. Thus, the study suggests that the green mediated ZnO-NPs could be used as an effective and eco-friendly alternative

in the removal of chemical contaminants, especially the azo dyes, from the polluted water.

ACKNOWLEDGMENT

This research did not receive any specific grant from funding agencies in the public, commercial, or not-for-profit sectors.

Conflict of interest

The author declare that we have no conflict of interest.

REFERENCES

1. El-Belely, E. F., Green synthesis of zinc oxide nanoparticles (Zno-nps) using arthrospira platensis (class: Cyanophyceae) and evaluation of their biomedical activities. *Nanomaterials.*, **2021**, *11*, 1-18.
2. Tettey, C. O. & Shin, H. M. Evaluation of the antioxidant and cytotoxic activities of zinc oxide nanoparticles synthesized using scutellaria baicalensis root. *Sci. African.,* **2019**, *6*, 1-7.
3. Sherafatkhah Azari, S.; Alizadeh, A.; Roufegarinejad, L.; Asefi, N. & Hamishehkar, H. Preparation and characterization of gelatin/ ßglucan nanocomposite film incorporated with ZnO nanoparticles as an active food packaging system. *J. Polym. Environ.*, **2021**, *29*, 1143-1152.
4. Elrefaey, A. A.; El-Gamal, A. D.; Hamed, S. M. & El-Belely, E. F. Algae-mediated biosynthesis of zinc oxide nanoparticles from Cystoseira crinite (Fucales; Sargassaceae) and it's antimicrobial and antioxidant activities. *Egypt. J. Chem.*, **2022**, *65*, 231-240.
5. Bekele, B. Green versus Chemical Precipitation Methods of Preparing Zinc Oxide Nanoparticles and Investigation of Antimicrobial Properties. *J. Nanomaterials.*, **2021**, 2021.
6. Becheri, A.; Dürr, M.; Lo Nostro, P. & Baglioni, P. Synthesis and characterization of zinc oxide nanoparticles: Application to textiles as UV-absorbers. *J. Nanoparticle Res.*, **2008**, *10*, 679-689.
7. Shao, F., Bio-synthesis of Barleria gibsoni leaf extract mediated zinc oxide nanoparticles and their formulation gel for wound therapy in nursing care of infants and children. *J. Photochem. Photobiol. B Biol.*, **2018**, *189*, 267-273.
8. Bhattacharya, P.; Mukherjee, D.; Deb, N.; Swarnakar, S. & Banerjee, S. Application of green synthesized ZnO nanoparticle coated ceramic ultrafiltration membrane for remediation of pharmaceutical components from synthetic water: Reusability assay of treated water on seed germination. *J. Environ. Chem. Eng.*, **2020**, *8*, 103803.
9. Chandra, H.; Patel, D.; Kumari, P.; Jangwan, J. S. & Yadav, S. Phyto-mediated synthesis of zinc oxide nanoparticles of Berberis aristata: Characterization, antioxidant activity and antibacterial activity with special reference to urinary tract pathogens. *Mater. Sci. Eng. Master Biol. Appl.*, **2019**, *102*, 212-220.
10. Shamhari, N. M.; Wee, B. S.; Chin, S. F. & Kok, K. Y. Synthesis and characterization of zinc oxide nanoparticles with small particle size distribution. *Acta Chim. Slov.*, **2018**, *65*, 278-585.
11. Lakshmana Naik Ramavathu.; Bala Narsaiah Tumma.; Ponniah Justin.; Photocatalytic degradation studies of malachite Green dye by hydrothermally synthesized Cobalt Vanadate nanoparticles, *Int. J. Nano. Dimens.,* **2023**, *14*(2), 145-156.
12 Gayathri1, S., Investigation of physicochemical properties of Ag doped ZnO nanoparticles prepared by chemical route. *Appl. Sci. Lett.,* **2015**, *1*, 8-13.
13. Mallakpour.; S. & Nouruzi.; N. Effect of modified ZnO nanoparticles with biosafe molecule on the morphology and physiochemical properties of novel polycaprolactone nanocomposites. *Polymer (Guildf).,* **2016**, *89*, 94-101.
14. Karam, S. T. & Abdulrahman, A. F. Green Synthesis and Characterization of ZnO Nanoparticles by Using Thyme Plant Leaf Extract. *Photonics.*, **2022**, *9*.
15. Balram Choudhary.; Anju Goyal.; Sukhbir L. Khokra.; P. New Visible Spectrophotometric Method for Estimation of itopride hydrochloride from tablets formulations using methyl orange reagent, *Journal, I. & Sciences.*, **2009**, *1*, 159-162.
16. Yu, J. & Yu, X. Hydrothermal synthesis and photocatalytic activity of zinc oxide hollow spheres. *Environ. Sci. Technol.*, **2008**, *42*, 4902-4907.

17. Song, J., Pathway and kinetics of malachite green biodegradation by Pseudomonas veronii. *Sci. Rep.*, **2020**, *11*, 1-11.
18. Nasuha, N., Effect of cationic and anionic dye adsorption from aqueous solution by using chemically modified papaya seed. *Int. Conf. Environ. Sci. Eng.*, **2011**, *8*, 50-54.
19. Lu, J., Photocatalytic degradation of methylene blue using biosynthesized zinc oxide nanoparticles from bark extract of Kalopanax septemlobus. *Optik (Stuttg).,* **2019**, *182*, 980-985.
20. Agarwal, H.; Venkat Kumar, S. & Rajeshkumar, S. A review on green synthesis of zinc oxide nanoparticles–An eco-friendly approach. *Resour. Technol.*, **2017**, *3*, 406-413.
21. Wigfield, A.; Eccles, J. & Rodriguez, D. Oops ! It looks like youre in the wrong. *Int. Bus. Res.*, **2013**, *3*, 404.
22. Baban, A.; Yediler, A. & Ciliz, N. K. Integrated water management and CP implementation for wool and textile blend processes. *Clean-Soil, Air, Water.*, **2010**, *38*, 84-90.
23. Ullah, R. & Dutta, J. Photocatalytic degradation of organic dyes with manganese-doped ZnO nanoparticles. *J. Hazard. Mater.*, **2008**, *156*, 194-200.
24. Narges Karimi.; Mandana Behbahani.; Ghasem Dini, and Amir Razmjou. Enhancing the secondary metabolite and anticancer activity of echinacea purpurea callus extracts by treatment with biosynthesized zno nanoparticles. *Advances in Natural Sciences: Nanoscience and Nanotechnology.*, **2018**, *9*(4), 045009,
25. Varadavenkatesan, T., Photocatalytic degradation of Rhodamine B by zinc oxide nanoparticles synthesized using the leaf extract of Cyanometra ramiflora. *J. Photochem. Photobiol. B Biol.*, **2019**, *199*, 111621.
26. Santos, S. A. O.; Freire, C. S. R.; Domingues, M. R. M.; Silvestre, A. J. D. & Neto, C. P. Characterization of phenolic components in polar extracts of eucalyptus globulus labill. Bark by high-performance liquid chromatography-mass spectrometry. *J. Agric. Food Chem.*, **2011**, *59*, 9386-9393.
27. Barzinjy, A. A. & Azeez, H. H. Green synthesis and characterization of zinc oxide nanoparticles using Eucalyptus globulus Labill. leaf extract and zinc nitrate hexahydrate salt. *SN Appl. Sci.*, **2020**, *2*, 1-14.
28. Muthu, N.; Lee, S. Y.; Phua, K. K. & Bhore, S. J. Nutritional, Medicinal and Toxicological Attributes of Star-Fruits (*Averrhoa carambola* L.): A Review. *Bioinformation.*, **2016**, *12*, 420-424.
29. Weng, Y., Functionalized gold and Silver bimetallic nanoparticles using Deinococcus radiodurans protein extract mediate degradation of toxic dye malachite green. *Int. J. Nanomedicine.,* **2020**, *15*, 1823-1835.
30. Annegowda, H. V.; Bhat, R.; Min-Tze, L.; Karim, A. A. & Mansor, S. M. Influence of sonication treatments and extraction solvents on the phenolics and antioxidants in star fruits. *J. Food Sci. Technol.*, **2012**, *49*, 510-514.
31. Neharkar, V. S. & Gaikwad, K. G. Hepatoprotective activity of Cassia alata(Linn.) leaves against paracetamol-induced hepatic injury in rats. *Res. J. Pharm. Biol. Chem. Sci.*, **2011**, *2*, 783-788.
32. Thirumavalavan, M.; Yang, F. M. & Lee, J. F. Investigation of preparation conditions and photocatalytic efficiency of nano ZnO using different polysaccharides. *Environ. Sci. Pollut. Res.*, **2013**, *20*, 5654-5664.
33. Pavan, F. A.; Mazzocato, A. C. & Gushikem, Y. Removal of methylene blue dye from aqueous solutions by adsorption using yellow passion fruit peel as adsorbent. *Bioresour. Technol.,* **2008**, *99*, 3162-3165.
34. Prado-Chay, D. A. Synthesis and Photocatalytic Activity of Cu2O Microspheres upon Methyl Orange Degradation. *Top. Catal.,* **2020**, *63*, 586-600.
35. Golmohammadi, M.; Honarmand, M. & Ghanbari, S. A green approach to synthesis of ZnO nanoparticles using jujube fruit extract and their application in photocatalytic degradation of organic dyes. Spectrochim. *Acta-Part A Mol. Biomol. Spectrosc.*, **2020**, 229.
36. Karimi, N.; Behbahani, M.; Dini, G. & Razmjou, A. Enhancing the secondary metabolite and anticancer activity of Echinacea purpurea callus extracts by treatment with biosynthesized ZnO nanoparticles. *Adv. Nat. Sci. Nanosci. Nanotechnol.*, **2018**, *9*.
37. Liu, Y. C., Biosynthesis of zinc oxide nanoparticles by one-pot green synthesis using fruit extract of Amomum longiligulare and its activity as a photocatalyst. *Optik (Stuttg).,* **2020**, 218.

38. Luque-Morales, P. A., Zno semiconductor nanoparticles and their application in photocatalytic degradation of various organic dyes. *Materials (Basel).,* **2021**, *14*.
39. Mohamed Isa, E. D., Che Jusoh, N. W., Hazan, R. & Shameli, K. Photocatalytic degradation of methyl orange using pullulan-mediated porous zinc oxide microflowers. *Environ. Sci. Pollut. Res.*, **2021**, *28*, 5774-5785.
40. He, Y., Highly efficient photocatalytic performance and mechanism of -ZnTcPc/g-C3N4 composites for methylene blue and tetracycline degradation under visible light irradiation. *Appl. Surf. Sci.*, **2019**, 498.
41. Gour, N. K.; Borthakur, K.; Paul, S. & Chandra Deka, R. Tropospheric degradation of 2-fluoropropene ($CH_3CF[dbnd]CH_2$) initiated by hydroxyl radical: Reaction mechanisms, kinetics and atmospheric implications from DFT study. *Chemosphere.*, **2020**, 238.
42. Manjari, G.; Saran, S.; Devipriya, S. P. & Rao, A. V. B. Novel Synthesis of Cu@ZnO and Ag@ ZnO Nanocomposite via Green Method: A Comparative Study for Ultra-Rapid Catalytic and Recyclable Effects. *Catal. Letters.*, **2018**, *148*, 2561-2571.
43. Gautam, R., Identification of Alcohol Effect Among Young Adults by Fourier Trans Infra Red (FTIR) *Spectroscopy*, **2011**, *2*, 624-635.
44. Shiv Shankar. Lily Jaiswal, R.S.L. Aparna, R. G. S. P. Synthesis, characterization, *in vitro* biocompatibility, and antimicrobial activity of gold , silver and gold silver alloy nanoparticles prepared from Lansium domesticum fruit, *Mater. Lett.*, **2014**, *137*, 75-78.
45. Karimi, J. & Mohsenzadeh, S. Rapid, green, and eco-friendly biosynthesis of copper nanoparticles using flower extract of Aloe vera. Synth. React. Inorganic, *Met. Nano-Metal Chem.*, **2015**, *45*, 895-898.
46. Siva, N.; Sakthi, D.; Ragupathy, S.; Arun, V. & Kannadasan, N. Synthesis, structural, optical and photocatalytic behavior of Sn doped ZnO nanoparticles. *Mater. Sci. Eng. B Solid-State Mater. Adv. Technol.*, **2020**, 253.
47. Kätzel, U.; Vorbau, M.; Stintz, M.; Gottschalk-Gaudig, T. & Barthel, H. Dynamic light scattering for the characterization of polydisperse fractal systems: II. Relation between structure and DLS results. Part. Part. Syst. *Charact.*, **2008**, *25*, 19-30.
48. Azizi, S.; Shahri, M. M. & Mohamad, R. Green synthesis of zinc oxide nanoparticles for enhanced adsorption of lead Ions from aqueous solutions: Equilibrium, kinetic and thermodynamic studies. *Molecules.*, **2017**, *22*.
49. Sundrarajan, M.; Ambika, S. & Bharathi, K. Plant-extract mediated synthesis of ZnO nanoparticles using Pongamia pinnata and their activity against pathogenic bacteria. *Adv. Powder Technol.*, **2015**, *26*, 1294-1299.
50. Sun, J. H.; Dong, S. Y.; Wang, Y. K. & Sun, S. P. Preparation and photocatalytic property of a novel dumbbell-shaped ZnO microcrystal photocatalyst. *J. Hazard. Mater.*, **2009**, *172*, 1520-1526.
51. Meena, S.; Vaya, D. & Das, B. K. Photocatalytic degradation of Malachite Green dye by modified ZnO nanomaterial. *Bull. Mater. Sci.*, **2016**, *39*, 1735-1743.
52. Nezamzadeh-Ejhieh, A. & Khorsandi, M. Heterogeneous photodecolorization of Eriochrome Black T using Ni/P zeolite catalyst. *Desalination.*, **2010**, *262*, 79-85.